

Ly α science from the LST aboard the ASO-S mission

Angelos Vourlidas

Johns Hopkins University Applied Physics Laboratory, Laurel, Maryland, USA; angelos.vourlidas@jhuapl.edu

Received 2019 June 28; accepted 2019 August 15

Abstract We review the status of solar Ly α science in anticipation of the upcoming Advanced Space-based Solar Observatory (ASO-S) mission, planned for a late 2021 (or 2022) launch. The mission carries a pair of the Ly α Solar Telescopes (LST) capable of high resolution disk and off-limb imaging, which will provide the first synoptic Ly α imaging observations of the solar atmosphere. We discuss the history of Ly α imaging and latest results, and outline the open questions that ASO-S could address. ASO-S will launch at an optimal time for Ly α science. Several other Ly α telescopes will be in operation. We identify the synergies between ASO-S and other missions as well as serendipitous non-solar science opportunities. We conclude that ASO-S has the potential for breakthrough observations and discoveries in the chromosphere-corona interface where the Ly α emission is the major player.

Key words: Sun: atmosphere — Sun: corona — Sun: UV radiation — Sun: activity — telescopes

1 INTRODUCTION

The Advanced Space-based Solar Observatory (ASO-S; Gan et al. 2015) aims to investigate how the solar magnetic field powers flares and coronal mass ejections (CMEs). These phenomena constitute the most powerful manifestations of energy release in our Solar System and can have profound effects on orbiting satellites and other technological systems on the Earth.

ASO-S is the first solar physics science mission in China to reach the engineering study phase (Phase-C/D) and is currently planned to launch in late 2021 or in 2022. The science payload consists of three instruments: a Full-disk vector MagnetoGraph (FMG), a Hard X-ray Imager (HXI), and the telescope suite of Ly α Solar Telescopes (LST; Li 2016). The instrument choice reflects the connection between the emergence of magnetic field through the photosphere into the corona where the explosive release of accumulated magnetic energy results in particle acceleration in flares (manifested as hard X-ray producing electrons) and magnetized plasma motion (manifested as CMEs). The objectives of the mission are discussed in more detail in Gan et al. (2015) and in <http://aso-s.pmo.ac.cn/english/index.php>. Here, we focus on the LST suite comprising a Solar Disk Imager (SDI), a Solar Corona Imager (SCI) and a full-disk White-light Solar Telescope (WST), see (Li & et al. 2019), for details. For reference, key performance parameters are summarized in Table 1, taken from table 4 in Li (2016). While

Table 1 Key Performance Parameters for the LST

	SDI	SCI
Wavelength	121.6 \pm 7.5 nm	121.6 \pm 10 nm
Field of view	0 – 1.2 R $_{\odot}$	1.1 – 2.5 R $_{\odot}$
Spatial Resolution	1.2''	4.8''
Temporal Resolution	4–40 s	15–60 s

the instrument performance is highly suited to explore dynamic phenomena, the LST suite is particularly novel for several other reasons. First, Ly α solar imaging observations are relatively rare. Second, it is the first time that on-disk and off-limb Ly α imagers are deployed together in space. Third, CME Ly α imaging is extremely rare, i.e., their coronal sources have never been imaged on disk. LST will open a new wavelength window on the Sun and therefore holds great promise for new discoveries.

Our aim with this paper is to put the anticipated LST science in context. In the rest of the paper, we review the status of solar Ly α on-disk (Sect. 2) and off-limb (Sect. 3) imaging as of this publication. We then proceed to discuss science synergies between LST and other Ly α telescopes and opportunities for non-solar science in Section 4 and conclude in Section 5.

2 OVERVIEW OF LY α DISK IMAGING

Solar disk Ly α observations have been traditionally undertaken with sounding rockets starting in 1956 (Mercure et al. 1956) followed by Purcell et al. (1959). The imag-

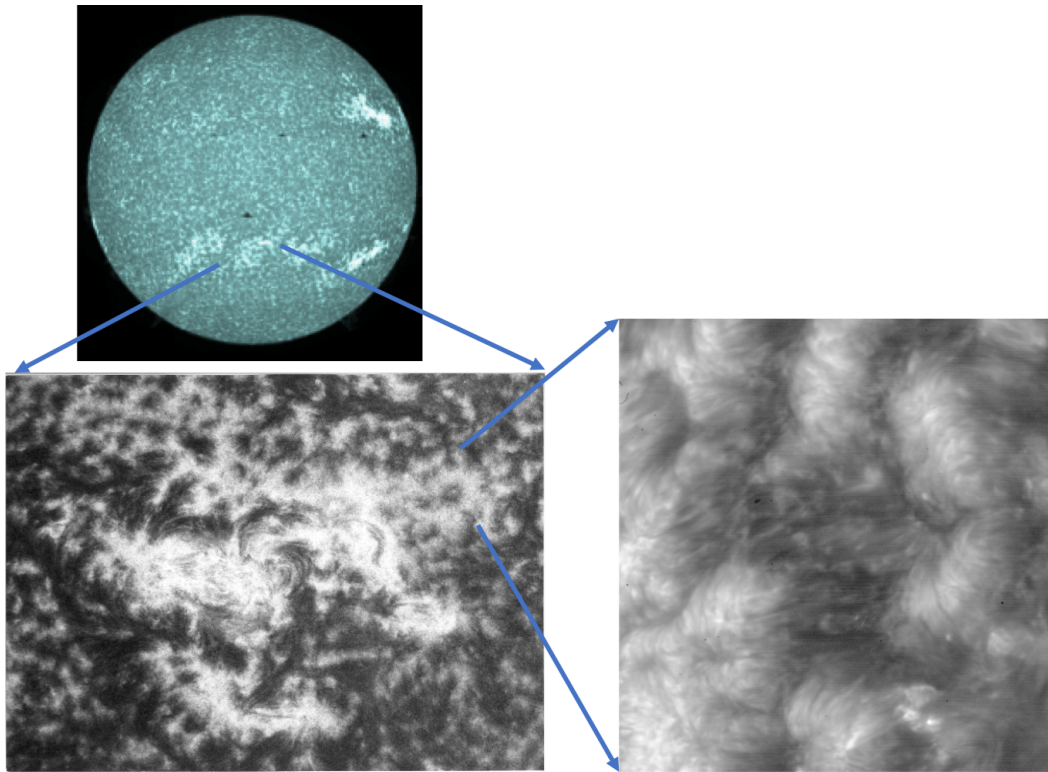


Fig. 1 The evolution of Ly α disk imaging through time. *Upper left*: Full disk image at 3'' resolution (From Prinz 1974). *Bottom left*: Active region imaged with TRC at 1'' resolution (From Bonnet et al. 1980). *Bottom right*: Network cell interior captured by VAULT at 0.3'' resolution (Adapted from Vourlidas et al. 2010). The *blue arrows* are intended to convey a sense of scale and time progression.

ing resolution, at a few arcmin, was coarse but sufficient to show emission from plages and absorption along long quiet Sun filaments. In 1972, Prinz (1973) obtained the images at 3'' resolution, which allowed the first detailed studies of the spatial distribution of Ly α on the disk (Prinz 1974) detecting the depletion of emission within the network cells and its enhancement along the internetwork lanes (Fig. 1, top left). The first arcsec time series were acquired in 1979 from the Transition Region Camera (TRC; Bonnet et al. 1980) revealing small-scale loops and threads throughout the network, seen both in emission and absorption (Fig. 1, bottom left). The 4-minute time series (the usual length of a sounding rocket flight) also suggested the dynamic nature of the emission with changes in emission occurring within a minute or so. Regular space-based disk imaging began with the launch of the Transition Region and Coronal Explorer (TRACE; Handy et al. 1999b) in 1998, which included a Ly α channel. Although the spatial resolution was high (about one arcsec), the emission was heavily contaminated with ultraviolet (UV) continuum emission, complicating the analysis. Initial efforts to model and remove the continuum were promising (Handy et al. 1999a), but the uncertainties, along with the difficulty in modeling and interpreting Ly α emission at the time, reduced Ly α observations to a context role. Very few published analy-

ses exist, mostly on flares (Rubio da Costa et al. 2009, and references therein).

Sub-arcsec imaging was finally achieved with a series of flights from the Very-high Angular resolution Ultraviolet Telescope (VAULT), achieving about 0.7 arcsec in its first flight (Korendyke et al. 2001) and 0.4 arcsec in its second one (Vourlidas et al. 2010, and Fig. 1, bottom right). The observations, extending over 5–6 min with a cadence of 17 s, were the first sub-arcsec images of solar structures in any wavelength (Fig. 2). The VAULT images avoid continuum contamination (they have 70% spectral purity) by employing gratings, rather than filters, to isolate a 150 Å bandpass around Ly α .

The VAULT images from the two flights revealed highly detailed loop structures over the network (Judge & Centeno 2008) and counter-flowing motions within filaments (Vourlidas et al. 2010). They enabled detailed studies of absorption and emission within a single filament (Vial et al. 2012) and of the thermal structure of spicules (Koza et al. 2009). The observations allowed detailed modeling of the radiative transfer as well (Patsourakos et al. 2007). Vourlidas et al. (2010) discuss in detail the observations and results from the two VAULT flights. The paper also provides a practical guide for interpreting Ly α disk images based on the ratio of Ly α intensities in different so-

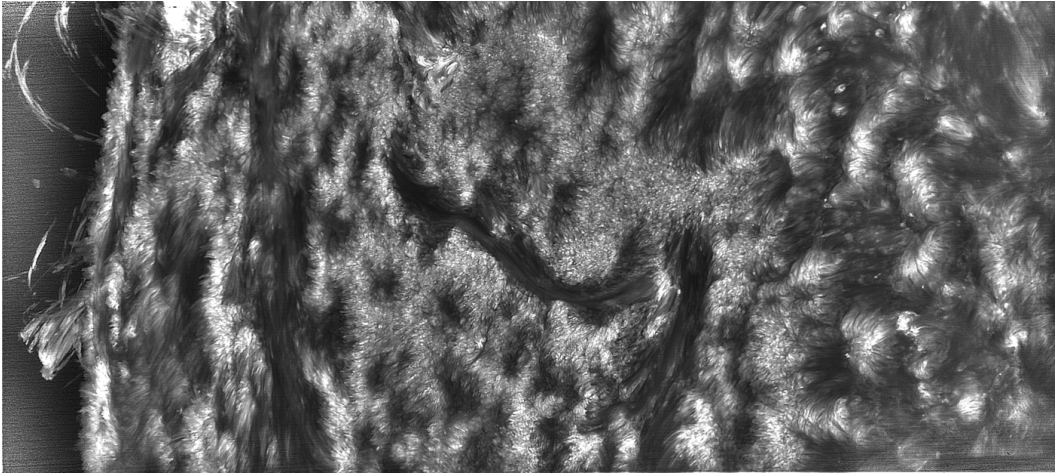


Fig. 2 Composite of the Ly α images acquired by the VAULT sounding rocket in May, 2001. It represents a $583'' \times 234''$ area of the northeastern quadrant at $0.3''$ resolution (423×170 Mm at 210 km resolution). The images were processed with a wavelet-based technique (Stenborg et al. 2008) to remove the diffuse stray light component and enhance the fine-scale structures.

lar structures relative to the quiet Sun. The so-called Ly α Relative Intensity (LRI) can be used to estimate the physical properties (temperature and densities ranges) in these structures (table 2 in Vourlidas et al. 2010).

The VAULT payload was upgraded and flown as VAULT2.0 in September 2014. While the cadence was improved to 6 s, detector problems reduced imaging resolution to the $2''$ level (Vourlidas et al. 2016). Nevertheless, interesting science was obtained thanks to the extensive observing campaign in support of the VAULT2.0 launch. Joint IRIS and Ly α observations drove a detailed simulation of the thermal structures of spicules, revealing that apparently high upflows seen in the lower transition region around spicules are thermal fronts and not real mass motions (Chintzoglou et al. 2018). This result may have important implications for the interpretation of small-scale activity at the crucial chromosphere-corona interface. The VAULT2.0 campaign captured a failed eruption in progress. Thanks to the availability of observational coverage from the photosphere to the corona, Chintzoglou et al. (2017) were able to demonstrate that the interaction of the erupting filament with the overlying magnetic topology was responsible for the failure of the eruption. These results shed fresh insights on the role of magnetic topology in eruptive activity. Nevertheless, much of the VAULT2.0 and accompanying campaign data, and much of the TRACE Ly α database for that matter, remain unexplored, leaving several open questions. We return to this issue in Section 4.

3 OVERVIEW OF LY α OFF-LIMB IMAGING

Coronal rain and partial loops are commonly seen over the limb within the limited ($< 0.1 R_{\odot}$ above the limb) field of view of disk imagers (e.g., Fig. 2). However, off-limb Ly α images at higher heights are rare and require corona-

graph designs to reject the bright emission from the disk. The first spatially resolved images were obtained from a sounding rocket, as flash spectra, during the 1970 March 7 solar eclipse (Speer & Garton 1970). The Ly α emission, detected up to about $1.8 R_{\odot}$, was shown to originate from resonant scattering of the chromospheric Ly α by photons by the small amount of remaining neutral hydrogen in the corona (fig. 5 in Gabriel 1971). Subsequently, the off-limb UV corona has been investigated spectroscopically in a sequence of occulted spectrographs on sounding rockets, the space shuttle and predominantly by the Ultraviolet Coronagraph Spectrometer (UVCS; Kohl et al. 1995) aboard the Solar and Heliospheric Observatory (SOHO; Domingo et al. 1995). The latter reconstructed full coronal images from multiple spectral scans once per day (Fig. 3). These images provided only the daily average state of the extended Ly α corona. Dynamic phenomena, such as waves, jets and CMEs, could be studied only through spectroscopy, with the large scale context missing. We will not discuss here the large body of literature on off-limb UV spectroscopy since it is not directly related to the LST. Interested readers are directed to Kohl et al. (2006) for an extensive review of off-limb Ly α spectroscopy and its history.

4 SCIENCE SYNERGIES AND NON-SOLAR SCIENCE

Despite the importance of Ly α emission in the chromosphere-corona dynamics, the science seems to be in limbo. There has been no disk imaging since the 2014 VAULT2.0 flight and no regular off-limb observations (imaging or spectroscopic) since the cease of UVCS operations in 2010. Thankfully, the situation will change with the launch of the ASO-S mission in late 2021 and the



Fig. 3 The Ly α off-limb corona as seen by UVCS reconstructed from spectral observations acquired during a period of several hours. Currently, there exists no capability to image the extended corona in Ly α . (Image source: <http://www.astro.wisc.edu/astro114/SOHO/971125/>).

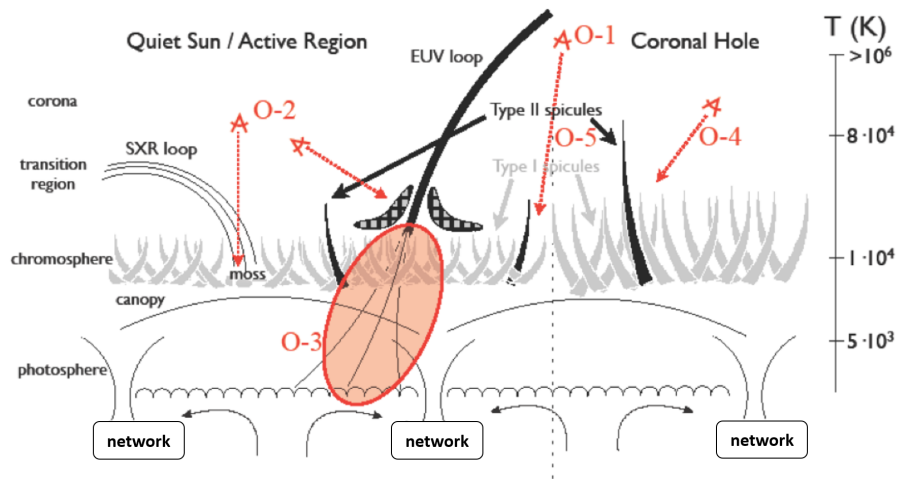


Fig. 4 Science targets (O-1 to O-4) for Ly α disk observations from future imagers, such as ASO-S/LST and/or Solar Orbiter/EUI. See Sect. 4 for details.

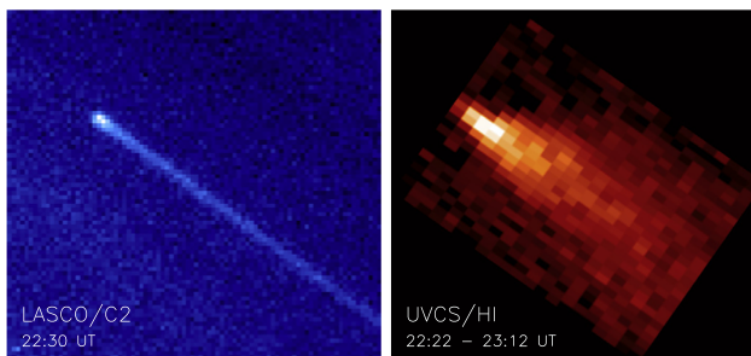


Fig. 5 Concurrent observations from LASCO and UVCS of the sungrazing comet C/2002 S2 showing the synergistic potential for off-limb Ly α imaging from LST/SCI. *Left panel:* details of visible light comet image from SOHO/LASCO C2 observation. *Right panel:* Ly α image reconstructed from SOHO/UVCS spectral observation. Image adapted from Bemporad et al. (2015).

deployment of LST. The two LST telescopes will finally offer regular synoptic imaging of the Ly α atmosphere, both on-disk and off-limb, with great spatial and temporal resolution (Table 1) for the first time.

Such highly-anticipated capability will finally allow us to address several lingering questions regarding the physics of the corona and solar wind. In the following, we offer a brief listing of science objectives (O-1 to O-5 in Fig. 4) where synoptic LST observations could make significant contributions.

O-1: What is the role of Type-II spicules in the transfer of energy and mass across the chromosphere-corona interface? The Hinode (Kosugi et al. 2007) Solar Optical Telescope (SOT; Tsuneta et al. 2008) discovered a new class of spicules, so-called Type-II spicules (de Pontieu et al. 2007). They have shorter lifetimes (10–150 s) than the “traditional” spicules and are observed in Ca II as thin jets (widths of 100–700 km or 0.1”–1”) shooting up in the atmosphere at high speeds (50–150 km s⁻¹). Preliminary results suggest that substantial heating occurs in Type-II spicules with some plasma reaching coronal temperatures. This may explain why the Type-II spicules disappear rapidly from the Ca II bandpass of SOT and may make them the ultimate source of coronal mass and heat (De Pontieu et al. 2009, 2011). Moreover, both spicule types seem to be constantly permeated by waves manifested as transverse oscillations of the order of 10–25 km s⁻¹ and periods of 100–500 s (de Pontieu et al. 2007; Langanen et al. 2008). The lack of photospheric contribution to the Ly α emission (compared to SOT Ca II observations) should result in superior visibility of the spicules in LST and the long time series should enable measurement of the amplitudes of transverse waves across a variety of magnetic field configurations and time scales, much more easily than with Hinode.

O-2: Does neutral plasma absorption of the extreme ultraviolet (EUV) emission from active region moss explain the discrepancies in the models of coronal loop heating? Moss is the bright, low-lying emission observed in many EUV images of solar active regions. These regions are considered the footpoints of high-temperature active region loops and can potentially provide valuable information on the conditions in high-temperature coronal loops (e.g., de Pontieu et al. 1999; Martens et al. 2000). Particularly, the moss intensity is predicted to be proportional to the total pressure in the coronal loop (Martens et al. 2000; Vourlidas et al. 2001), which is an important constraint for coronal loop modeling. Current models, however, largely overestimate the EUV emission of the moss relative to that of the overlying loops. De Pontieu et al. (2009) suggest that the disagreement partly arises from absorption of the moss EUV radiation by neutral

plasma at the same height. VAULT limb images (Fig. 2 and Vourlidas et al. 2010) clearly show that cool Ly α emission (in the form of coronal rain) exists at coronal heights of 80” (56 000 km). By using Ly α as a tracer of neutral hydrogen, LST can provide vital evidence of the presence and mixing of neutral plasma at the height where EUV highly ionized emission is observed by EIS and SDO/AIA. By identifying HI structures in the moss regions, LST will detect absorption of EUV moss emission at the same spatial scales as AIA and provide a means of quantifying the amount of absorbed radiation using detailed models (e.g., Gouttebroze 2006). Moreover, detailed comparisons between Ly α structures and EUV moss for a wide range of lines of sight, from disk center to limb, can provide critical information on the geometry, filling factor and in general about the mixing of cool and hot material in and around the footpoints of active region loops. Such observations will help us understand where the EUV emission originates on small scales – e.g., next to or on top of dynamic fibrils.

O-3: Where are the chromospheric footpoints of coronal loops? Since energy cannot be produced in the corona itself, it has to be transported from below, and the chromosphere is a natural gateway for its transmission. Understanding the connection between solar coronal structures to the photospheric magnetic field is of crucial importance for understanding the mechanisms that channel mass and energy from the solar interior to the corona. Attempts at associating individual loop structures to magnetic field elements in the photosphere have failed, largely because of the difficulty in visually connecting coronal loop structures to transition region, chromospheric and photospheric signatures (Landi & Feldman 2004). Current models of coronal loops fail at predicting the correct level of transition region and chromospheric emission, overestimating it by a factor 10 or more. Yet, the physics of the chromospheric portion of a loop is fundamental in determining the temperature, emission measure and density structure in its coronal section. For example, wave heating propagation strongly depends on the temperature and density stratification of low-temperature loop plasma – yet no observational constraints can be provided. The almost isothermal temperature profile of the coronal section of loops and its peak value are not reproduced by current theoretical loop models; however, Landi & Feldman (2004) showed that a reduction in the cross section of a loop at chromospheric temperatures could yield shapes and values in much closer agreement with observations. Yet, the determination of the cross-sectional variation of a loop at heights in the chromosphere escapes us. LST will have equal or higher spatial resolution than the photospheric and coronal observations and will routinely extend over a significant fraction of the coronal loop lifetime (\approx 1000 s).

O-4: What is the structure of coronal holes in the Ly α temperature range? The VAULT flights revealed plasma structures in the dark cell interiors, as well as extreme filamentation in the network lanes (Fig. 1 and Vourlidas et al. (2010)). No such observations have been made in coronal holes at high spatial resolution but they can potentially address several key open problems. For example, Feldman et al. (2009) found out that the plasma distribution with temperature in the transition region of coronal holes, the quiet Sun and active regions was the same, decreasing steadily with temperature with a fixed slope. No apparent difference was visible between those regions, and within those regions (i.e., network and intranetwork), indicating that the differentiation between coronal holes, quiet Sun and active region in the upper atmosphere initiates at temperatures larger than 30 000 K (see also Patsourakos et al. 1999). The analysis of Feldman et al. (2009) was, however, confined to plasmas with temperatures of $2 \times 10^4 - 2 \times 10^5$ K. On the contrary, H α line center images show a very big difference in appearance between coronal holes and the quiet Sun, with the canopy-like structures becoming less apparent in coronal holes. Rather surprisingly, equatorial coronal holes appear brighter than the surrounding quiet Sun in Ly α and other chromospheric lines (Bocchialini & Vial 1996). *Is the Ly α chromosphere sharing the same behavior as the H α images, or as the transition region plasma? Do coronal holes have the same chromospheric structures as the quiet Sun?* The relationship between coronal hole large-scale structures—the plumes—and the chromosphere also needs to be investigated. The Hinode/XRT imager unveiled the presence of ubiquitous X-ray jets that populate coronal holes, originating in bright points scattered across the entire polar coronal hole area and many of them are associated with coronal plumes (Raouafi et al. 2016, and references therein). Such jets are believed to be the result of magnetic reconnection, but little is known regarding the origin of the reconnecting plasmas, and their relationship to chromospheric emission. LST, using both SDI and SCI, can target coronal holes and acquire long time series (i.e., several hours to match the typical lifetime (100–2000s) of a polar jet) of many jets.

O-5: What is the H density and other element abundances at the base of the solar wind? The source regions of the fast and slow solar wind are only known in poor detail: the former originates from coronal holes, and the latter from quiet equatorial streamers. The exact position of wind sources within such regions is, however, not yet known, except that it is located below $2 R_{\odot}$, but it can have a crucial impact on models of solar wind acceleration. The absolute elemental composition of off-disk coronal plasmas is known to be one of the most powerful tracers of solar wind origin (Feldman et al. 2005;

Laming et al. 2019), but reliable measurements are scarce, mostly because of the difficulty of detecting local coronal HI emission below $1.5 R_{\odot}$ to measure absolute element abundances. The high sensitivity of LST/SCI should allow detecting the off-disk coronal Ly α emission that, coupled with disk or off-limb high resolution spectra (e.g., from EIS or the Solar Orbiter SPICE spectrometer), will enable direct absolute abundance measurements of key elements, aiding in discriminating the source regions of the solar wind down to arcsec-level scales. The observations of the quiet Sun/coronal hole boundary will determine elemental abundances in the source regions of both kinds of wind, and to study the boundary where the transition between the two wind regimes occurs.

4.1 Science Synergies

The deployment of LST in 2021 comes at a fortuitous time for Ly α science. The Solar Orbiter mission (Müller et al. 2013) is scheduled to launch in February 2020 with regular imaging observations starting in March 2021. The spacecraft carries two telescopes with Ly α capabilities. The Extreme Ultraviolet Imager (EUI; Halain et al. 2014) will observe the solar atmosphere with a 1000 arcsec field of view in two channels, Ly α and 174 Å. The Multi Element Telescope for Imaging and Spectroscopy (METIS; Romoli et al. 2017) is a dual visible light and Ly α coronagraph with a 3° field of view. The EUI and METIS nicely complement the SDI and SCI telescopes, respectively, and can result in strong synergies. But first, the unusual Solar Orbiter concept of operations needs to be considered. Solar Orbiter will be launched into an inclined inner heliospheric orbit with minimum perihelion of 0.28 AU, and aphelion at 0.8 AU. Through a sequence of Venus gravity assists, it will raise its inclination from a few degrees in 2021 to 34° by 2027, providing unprecedented views of the solar poles. However, the highly elliptical orbit comes with power and telemetry constraints, which restrict the science operations for the imaging instruments to three 10-day windows for each 168-day orbit. Therefore, EUI and METIS will image, albeit intermittently, the Ly α Sun for wildly different longitudinal and latitudinal viewpoints compared to LST.

These configurations can greatly extend the study of the objectives we discussed previously (Fig. 4). For example: (1) they allow 3-D reconstructions of various features from loops to large filaments (O-1); (2) they can readily extract the contribution of moss via simultaneous imaging of the same structures (O-2); (3) they can facilitate the study of polar coronal holes and high-latitude filaments by avoiding the line-of-sight effects that plague ecliptic-based telescopes; (4) they can help trace the outflow of neutral plasma from the surface to the solar wind. This is just a

small collection of possible synergies for solar studies with Solar Orbiter.

Further synergistic opportunities exist for eruptive event studies, such as CMEs flares, and solar energetic particles. The Ultraviolet Spectro-Coronagraph Pathfinder (UVSC; Strachan et al. 2017) will perform detailed measurements of the Ly α line profile in the off-limb corona. Any deviations from a Maxwellian (Gaussian) shape will signal the presence of non-thermal particle populations, which are regularly invoked in theories of particle acceleration as the seed (or ‘precursor’) particles. The experiment will launch into a geosynchronous orbit no earlier than August 2020. UVSC will obtain spectra simultaneously at two heights (1.8 and 3 R $_{\odot}$) with a spatial resolution of 10 and 42 arcsec, respectively. Thanks to its complimentary field of view, LST/SCI can provide the large-scale context for the UVSC spectra observations and help pinpoint the site of the seed particles while the SDI observations can link those particles to any flaring or eruptive activity. The SDI/SCI combination may be instrumental in deciphering the origin and time history of seed particles and their spatial relation to the CME and shock. Such information can advance our ability to predict SEPs and enhance the operational utility of both UVSC and ASO-S. Since eruptive activity is difficult to predict in advance, CME synergies with Solar Orbiter will require some luck, but it will be prudent to develop CME-specific observing plans and coordination between ASO-S and the Solar Orbiter teams (particularly, SPICE, EUV and METIS), well in advance.

4.2 Non-Solar Science

Solar science is not the only science that LST can contribute to. As demonstrated by SOHO, Ly α observations of comets are possible and can lead to important science (e.g., Mäkinen et al. 2001; Bemporad et al. 2015). They can help derive the water content, size and tail composition of the target and can use the target to probe the density, temperature and velocity of the near-Sun solar wind (see Bemporad et al. 2015, and references therein).

Another possible target, if the SCI sensitivity allows it, is the auroras on Jupiter and Saturn (Nichols et al. 2007). Although SCI cannot spatially resolve the emission, it may be able to detect enhancements in the UV aurora of Jupiter (and maybe Saturn, if long exposures and stable pointing can be achieved). Given the very limited availability of Hubble Space Telescope time, the LST observations could be the only way to study those auroras during the Cycle 25 solar maximum.

Finally, the LST synoptic observations will be welcomed for Sun-Earth studies. It is well-known that solar Ly α variations modulate the chemistry of the mesosphere

(e.g., ozone layer) and can affect the climate on longer time scales. The lack of spatially resolved Ly α time series limits our understanding of the origins of those variations and hinders our ability to predict them. LST will provide, for the first time, a synoptic and detailed map of extents, intensities and evolution of the solar source of Ly α emission. Such information should clarify where the Ly α variations arise, which are the most important solar sources and possibly aid in the development of more accurate indices for use in models of the terrestrial atmosphere and for space weather purposes. To be useful in irradiance studies, however, the SDI observations need to be calibrated carefully and reliably. The simultaneous operations of the other Ly α instruments we mentioned above, such as EUV and possibly the Extreme Ultraviolet Variability Experiment (EVE; Woods et al. 2012), should provide cross-calibration opportunities. Sounding rocket underflights, with well-calibrated Ly α instruments, e.g., an SDI flight spare, for example, could also be considered.

5 CONCLUSIONS

This paper aims to provide a concise overview of the status of Ly α solar imaging, open questions and synergistic science opportunities for LST as ASO-S enters its development phase. It is clear that LST will close a long-term gap in the observations and understanding of a crucial component of the solar atmosphere. The LST synoptic on-disk and off-limb observations will finally help us understand the sources of Ly α emission on the Sun, and elucidate the flow of energy from the chromosphere to the corona. Further out, H abundance measurements along with the speeds of outflowing cool material will provide key constraints to theories of the solar wind. In CMEs and flares, LST will allow us to study the role of cold plasmas within CMEs and help us understand particle acceleration in flares. As we discussed in the previous sections, we expect LST to play a role in such extensive science, from the physics of comets to atmospheric studies at the Earth. The community is looking forward to the successful launch of ASO-S and the deployment of LST.

Acknowledgements This work was supported by NRL (Grant N00173-16-1-G029). The VAULT2.0 development was funded by the NASA H-TiDeS program under NNG12WF671. The author is grateful to Prof. Weiqun Gan, Dr. Hui Li and the LST team at Purple Mountain Observatory for their hospitality.

References

Bemporad, A., Giordano, S., Raymond, J. C., & Knight, M. M. 2015, *Advances in Space Research*, 56, 2288

- Bocchialini, K., & Vial, J.-C. 1996, *Sol. Phys.*, 168, 37
- Bonnet, R. M., Decaudin, M., Bruner, Jr., et al. 1980, *ApJ*, 237, L47
- Chintzoglou, G., De Pontieu, B., Martínez-Sykora, J., et al. 2018, *ApJ*, 857, 73
- Chintzoglou, G., Vourlidas, A., Savcheva, A., et al. 2017, *ApJ*, 843, 93
- de Pontieu, B., Berger, T. E., Schrijver, C. J., & Title, A. M. 1999, *Sol. Phys.*, 190, 419
- De Pontieu, B., Hansteen, V. H., McIntosh, S. W., & Patsourakos, S. 2009, *ApJ*, 702, 1016
- de Pontieu, B., McIntosh, S., Hansteen, V. H., et al. 2007, *PASJ*, 59, 655
- De Pontieu, B., McIntosh, S. W., Carlsson, M., et al. 2011, *Science*, 331, 55
- Domingo, V., Fleck, B., & Poland, A. I. 1995, *Sol. Phys.*, 162, 1
- Feldman, U., Dammasch, I. E., & Landi, E. 2009, *ApJ*, 693, 1474
- Feldman, U., Landi, E., & Schwadron, N. A. 2005, *Journal of Geophysical Research (Space Physics)*, 110, A07109
- Gabriel, A. H. 1971, *Sol. Phys.*, 21, 392
- Gan, W., Deng, Y., Li, H., et al. 2015, in *Society of Photo-Optical Instrumentation Engineers (SPIE) Conference Series*, 9604, Proc. SPIE, 96040T
- Gouttebroze, P. 2006, *A&A*, 448, 367
- Halain, J. P., Rochus, P., Renotte, E., et al. 2014, in *SPIE Conference Series*, 9144, 914408
- Handy, B. N., Tarbell, T. D., Wolfson, C. J., Korendyke, C. M., & Vourlidas, A. 1999a, *Sol. Phys.*, 190, 351
- Handy, B. N., Acton, L. W., Kankelborg, C. C., et al. 1999b, *Sol. Phys.*, 187, 229
- Judge, P., & Centeno, R. 2008, *ApJ*, 687, 1388
- Kohl, J. L., Noci, G., Cranmer, S. R., & Raymond, J. C. 2006, *A&A Rev.*, 13, 31
- Kohl, J. L., Esser, R., Gardner, L. D., et al. 1995, *Sol. Phys.*, 162, 313
- Korendyke, C. M., Vourlidas, A., Cook, J. W., et al. 2001, *Sol. Phys.*, 200, 63
- Kosugi, T., Matsuzaki, K., Sakao, T., et al. 2007, *Sol. Phys.*, 243, 3
- Koza, J., Rutten, R. J., & Vourlidas, A. 2009, *A&A*, 499, 917
- Laming, J. M., Vourlidas, A., Korendyke, C., et al. 2019, *ApJ*, 879, 124
- Landi, E., & Feldman, U. 2004, *ApJ*, 611, 537
- Langangen, Ø., Carlsson, M., Rouppe van der Voort, L., Hansteen, V., & De Pontieu, B. 2008, *ApJ*, 673, 1194
- Li, H. 2016, in *IAU Symposium*, 320, *Solar and Stellar Flares and their Effects on Planets*, eds. A. G. Kosovichev, S. L. Hawley, & P. Heinzel, 436
- Li, H., Chen, B., Feng, L., et al. 2019, *RAA (Research in Astronomy and Astrophysics)*, 19, 158
- Mäkinen, J. T. T., Bertaux, J.-L., Pulkkinen, T. I., et al. 2001, *A&A*, 368, 292
- Martens, P. C. H., Kankelborg, C. C., & Berger, T. E. 2000, *ApJ*, 537, 471
- Mercure, R., Miller, Jr., S. C., Rense, W. A., & Stuart, F. 1956, *J. Geophys. Res.*, 61, 571
- Müller, D., Marsden, R. G., St. Cyr, O. C., & Gilbert, H. R. 2013, *Sol. Phys.*, 285, 25
- Nichols, J. D., Bunce, E. J., Clarke, J. T., et al. 2007, *Journal of Geophysical Research (Space Physics)*, 112, A02203
- Patsourakos, S., Gouttebroze, P., & Vourlidas, A. 2007, *ApJ*, 664, 1214
- Patsourakos, S., Vial, J.-C., Gabriel, A. H., & Bellamine, N. 1999, *ApJ*, 522, 540
- Prinz, D. K. 1973, *Sol. Phys.*, 28, 35
- Prinz, D. K. 1974, *ApJ*, 187, 369
- Purcell, J. D., Packer, D. M., & Tousey, R. 1959, *Nature*, 184, 8
- Raouafi, N. E., Patsourakos, S., Pariat, E., et al. 2016, *Space Sci. Rev.*, 201, 1
- Romoli, M., Landini, F., Antonucci, E., et al. 2017, in *Society of Photo-Optical Instrumentation Engineers (SPIE) Conference Series*, 10563, 105631M
- Rubio da Costa, F., Fletcher, L., Labrosse, N., & Zuccarello, F. 2009, *A&A*, 507, 1005
- Speer, R. J., & Garton, W. R. S. 1970, *Nature*, 226, 249
- Stenborg, G., Vourlidas, A., & Howard, R. A. 2008, *ApJ*, 674, 1201
- Strachan, L., Laming, J. M., Ko, Y.-K., et al. 2017, in *AAS/Solar Physics Division Meeting*, Vol. 48, *AAS/Solar Physics Division Abstracts #48*, 110.07
- Tsuneta, S., Ichimoto, K., Katsukawa, Y., et al. 2008, *Sol. Phys.*, 249, 167
- Vial, J. C., Olivier, K., Philippon, A. A., Vourlidas, A., & Yurchyshyn, V. 2012, *A&A*, 541, A108
- Vourlidas, A., Klimchuk, J. A., Korendyke, C. M., Tarbell, T. D., & Handy, B. N. 2001, *ApJ*, 563, 374
- Vourlidas, A., Sanchez Andrade-Nuño, B., Landi, E., et al. 2010, *Sol. Phys.*, 261, 53
- Vourlidas, A., Beltran, S. T., Chintzoglou, G., et al. 2016, *Journal of Astronomical Instrumentation*, 5, 1640003
- Woods, T. N., Eparvier, F. G., Hock, R., et al. 2012, *Sol. Phys.*, 275, 115